# 2. Semester Project FT-506
# Chaos Theory

05.27.24

**Kristoffer T. Nielsen, Mikkel B. Øbro & Palo H. Khalil**
*Supervisors:*
*Lars Folke Olsen*
*Adam Cohan Simonsen*
*Michael Andersen Lomholt*

**SDU✸**

# Contents

# Abstract

*Chaotic systems are a fascinating aspect of the more broad topic nonlinear dynamics. Chaos is characterized by sensitivity to initial conditions and complex behaviors, that appear random yet exhibit underlying order. The purpose of this report is to analyze this behavior in an oscillating mechanical system, while drawing similarities to the numerical solutions. Connecting this with an analogy between the chaos in our specific system and the application to the real world*

# 1 Introduction

Many people might be familiar with the word 'chaos', since it seems to be almost everywhere. The term *Butterfly effect* is a very known phenomena, describing the fundamental meaning of chaos. The butterfly effect describes the "cause and effect" concept, where one event leads to another. "A flap from a butterfly in Brazil sets of a tornado in Texas.", this sentence states that small changes can generate a ripple effect, causing big changes. In classical physics, a system is deemed 'deterministic', stating that the future state of the system is determined by the current condition of the system. This explains why the path of a ball thrown in the air can be predicted, or the orbital path of a planet around the sun. All classical systems are deterministic, but yet many of them are unpredictable under certain circumstances. Systems that contain this kind of behavior are 'chaotic'. Chaos is characterized by the sensitivity to the initial conditions, where small uncertainties make the outcome unpredictable. The purpose of this report is to get an understanding of this chaotic behavior, and how to analyze such systems. This report will do this by looking at the traditional torsion pendulum, a comprehendible mechanical system. But by adding an extra mass, the motion develops from very simple, to a chaotic and unpredictable motion. An analysis of the system using both empirical data and numerical simulations will be made. By comparing the observed behavior with the predicted outcomes from mathematical models. Specifically looking at many different diagrams for both the experiment and numerical solution. Diagrams such as the angle plot is examined, known to be described by a sine wave for the traditional pendulum. This is not the case for a chaotic system, since it will never repeat. When working with non repeating systems, the phase space diagram is interesting to look at. This plot tells the relation between the angle and the angular velocity, used to see chaotic behaviour for complex motion for the torsion pendulum. With relation to the phase space, the Poincaré plot/diagram will be examined. This takes a point in the phase space for every period, creating a fascinating pattern called a fractal, which is a never ending pattern. And in this context the fractal dimension of the Poincaré plots will be calculated. The transition between periodic motion and chaos, is another thing to look at. This is done by varying one of the parameters, and looking at the effect on the Poincaré plot, doing this a bifurcation diagram can be made. Lastly an analogy of the concept chaos will be drawn between our system and real world applications.
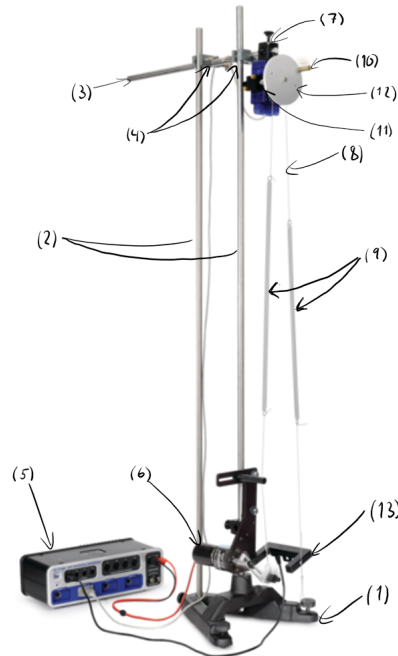
# 2   Torsion pendulum

## 2.1   Setup



Figure 1: Setup of mechanical system

(1) Large Rod Stand (ME-8735)

(2) 120 cm Long Steel Rod (2 pcs.) (ME-8741)

(3) 45 cm Long Steel Rod (ME-8736)

(4) Multi Clamps (2 pcs.) (ME-9507)

(5) 850 Universal Interface (UI-5000)

(6) Mechanical Oscillator/Driver (ME-8750)

(7) Rotary Motion Sensor (PS-2120)

(8) String

(9) spring (CI-6689A)

(10) Mass (CI-6689A)

(11) magnet (CI-6689A)

(12) Disc (CI-6689A)

(13) Photogate Head (ME-9498A)

(14) Caliper

(15) Scissors

(16) PASCO Capstone Software (UI-5400)

(17) MatLab Software

## 2.2   System analysis

In this report, the system seen on figure (1) is examined. A free body diagram is made to analyze the motion of the pendulum more easily:
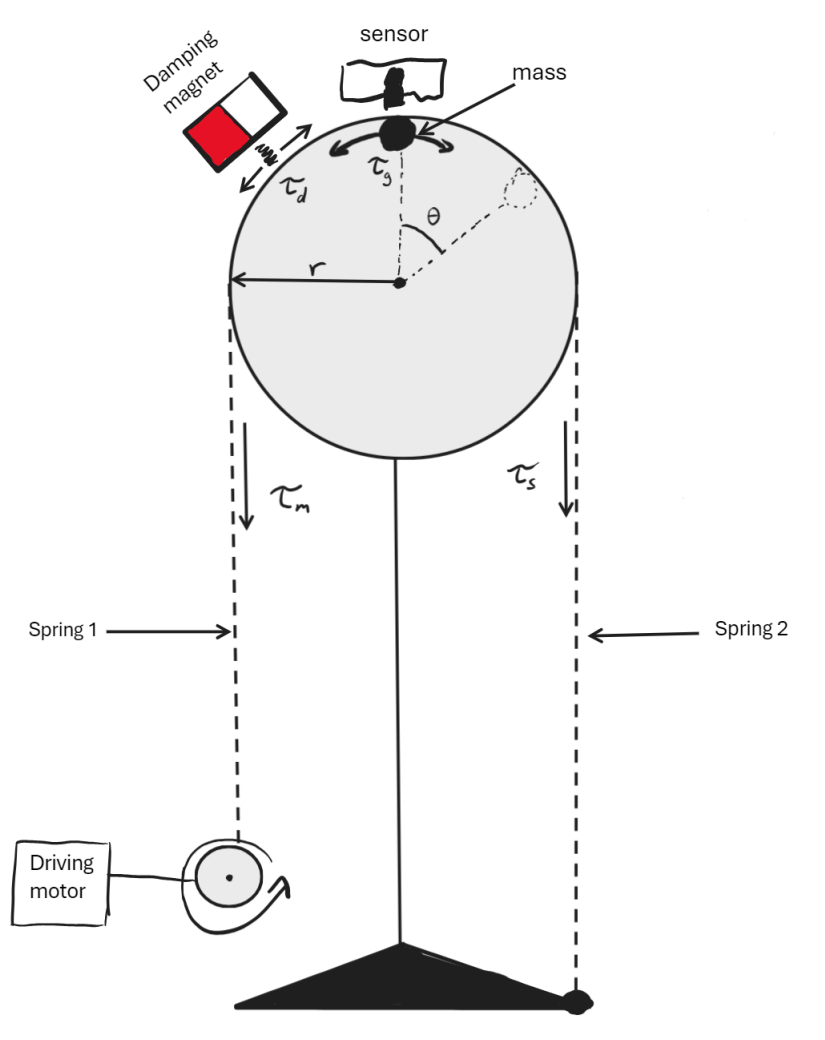


Figure 2: Free body diagram of the torsion pendulum

To predict the motion of the system, we need to describe the motion using differential equations. We know according to Newtons second law of motion for rotation:

$$\sum_i \tau_i = I\alpha \tag{1}$$

where $\alpha = \frac{d^2\theta}{dt^2}$ and $I$ is the inertia of the pendulum, which is described using:

$$I = \frac{1}{2}m_{disc}r^2 + mr^2 \tag{2}$$

Here, $m_{disc}$ is the mass of the disc and $m$ is the mass of the lot attached to the disc. $r$ is the radius

of the disc, which is the same distance as to where the lot is located (not correctly represented in figure (2))

The magnetic torque depend on the angular velocity of the pendulum, thus the damping torque is described by:

$$\tau_d = -\gamma \frac{d\theta}{dt} \tag{3}$$

From equation (3) the parameter $'\gamma'$ describes the damping coefficient. The closer the magnet, the bigger the value, and note that friction also contributes to this value.

The springs is affected by Hooke's law as

$$\tau_s = -\kappa\theta \tag{4}$$

The description for the gravitational torque caused by the point mass.

$$\tau_g = mgrsin(\theta) \tag{5}$$

This force will always act in the opposite direction to the others, thus it must have a positive sign. Lastly the driving torque is just explained by a cosine wave as:

$$\tau_m = A_0 cos(\omega_d t) \tag{6}$$

For a better notation we introduce $\dot{\theta}$, which is equivalent to $\frac{d\theta}{dt}$. Another dot is added for the second derivative, thus we also get $\alpha = \ddot{\theta}$. From equation (1), the following equation can be written to describe the motion of the pendulum:

$$I\ddot{\theta} = \tau_d + \tau_s + \tau_g + \tau_m \tag{7}$$

This is rearranged to get:

$$I\ddot{\theta} + \gamma\dot{\theta} + \kappa\theta - mgrsin(\theta) = A_0 cos(\omega_d t) \tag{8}$$

To see how the system has two equilibrium positions, it can easily be visualized, when looking at the potential $(U_p(\theta))$ graph of the system:

$$U_p(\theta) = -\int \tau_s + \tau_g \, d\theta = -\int -\kappa\theta + mgrsin(\theta) \, d\theta = \frac{1}{2}\kappa\theta^2 + mgrcos(\theta) \tag{9}$$
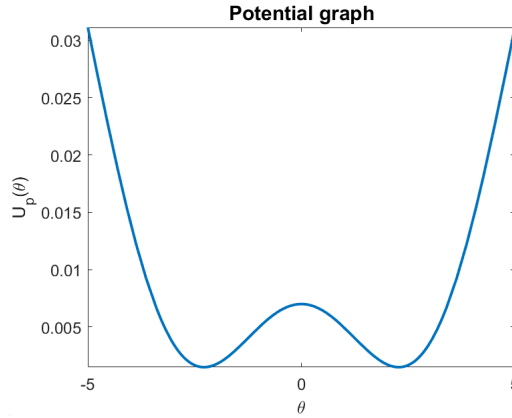
visualized as:

Figure 3: Graph showing the 'double well' potential of our system

From this, it is seen that the pendulum has two stable stationary points, in the bottom of each 'well'. This corresponds to the points at which the gravitational torque and the spring torque cancels out. Another unstable stationary point is seen from figure (3) at $\theta = 0$. This is when the point mass is at the top of the pendulum, and the spring torque is zero, since both springs pull with the same torque.

# 3 Experiment and Results

## 3.1 Determine coefficients

To analyze the system, a value for each parameter shall be calculated. Giving the values used to solve the differential equation numerically. The parameters can be calculated in the following way:

### 3.1.1 Inertia (I)

To determine the inertia, it is assumed that the mass of the disc is distributed evenly, and the applied mass can be assumed as a point mass from the center. These assumptions gives us the following expression for the inertia

$$I = \frac{1}{2} \cdot m_{disc} \cdot r^2 + m_{mass} \cdot r^2 \tag{10}$$

the following measurements were made to calculate the inertia

|  | measurement |
|---|---|
| $m_{disc}$ | 121.92 g |
| $m_{mass}$ | 14.8502 g |
| $r$ | 4.8 cm |

Table 1: Inertia measurements

7

The inertia can be calculated:

$$I = \frac{1}{2} \cdot 0.12192\,kg \cdot (0.048\,m)^2 + 0.0148502\,kg \cdot (0.048\,m)^2 = 1.7467 \cdot 10^{-4} kg \cdot m^2 \qquad (11)$$

### 3.1.2   Angular frequency of driving torque ($\omega_d$)

This can easily be measured with the photogate, to get the driving frequency as a function of voltage. To get a direct translation from voltage to angular frequency ($\omega_d$), the driver can be set to a up- or down-ramp, by plotting the voltage and $\omega_d$ value. Angular frequency is calculated in the software as: $\omega_d = \frac{2\pi}{Period(s)}$ giving us the following graph:
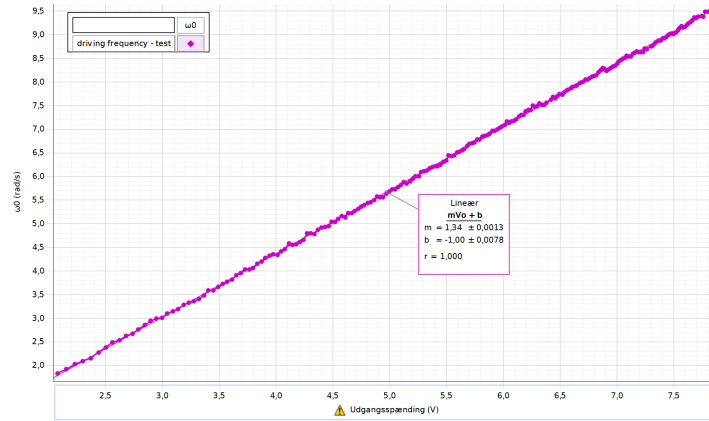


Figure 4: Graph showing the relation between driver voltage and driving frequency

From figure (4), it is seen that the value of $\omega_d$ with relation to the voltage input ($U_e$) of the motor, is given by

$$\omega_d = 1.34 \cdot U_e - 1 \qquad (12)$$

This equation is used to determine which $\omega_d$ value is used when driving the motor.

### 3.1.3   Spring constant ($\kappa$)

To determine spring constant ($\kappa$), the mass is taken of. A lot is attached to one of the springs in the system shown on figure 2. From this, equation (8) can be rewritten, since there is no driven force and no velocity

$$\kappa\theta = m_{lot}gr_i$$

$$\kappa = \frac{m_{lot}gr_i}{\theta} \qquad (13)$$

The mass of the lot ($m_{lot}$) used is measured to be 21 g, the radius rotation ($r_i$ the radius where the string rotates) is measured as 2.2 cm. The resulting angle is extracted from the data:
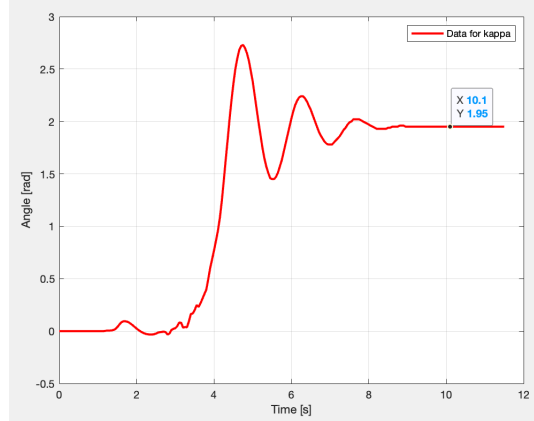
Figure 5: Graph showing the angle difference, when a lot is attached to the spring

From figure (5) the resulting angle is measured to be 1.95 radians. Now all values can be plugged into the equation (13)

$$\kappa = \frac{2.1 \cdot 10^{-2}\, kg \cdot 9.82\, \frac{m}{s^2} \cdot 2.2 \cdot 10^{-2}\, m}{1.95\, rad} = 2.33 \cdot 10^{-3} N \cdot m \cdot rad^{-1} \tag{14}$$

### 3.1.4   Damping coefficient ($\gamma$)

To determine Damping coefficient ($\gamma$), the mass is taken off since it is easier to fit a function to the graph, when no mass is in the system. The magnet is set to a desired distance, for our case it was screwed all the way back. The disc is turned from the equilibrium, and data for five different graphs is found, to get an accurate average:
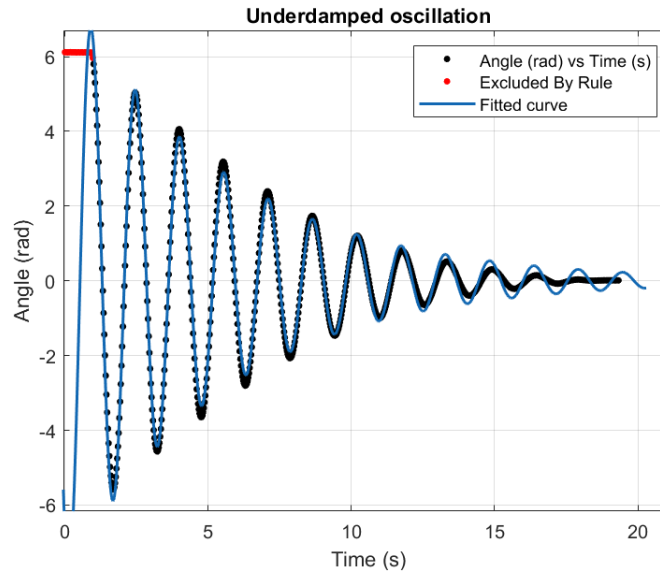


Figure 6: Fitted curve to underdamped harmonic oscillation

The curve is fitted using:

$$f(x) = ae^{-bx} sin(\omega_0 x + \phi) + k \tag{15}$$

9

Where the value of $b$ is given as $\frac{\gamma}{2I_n}$, which is derived for the under damped harmonic oscillation [2]. It is important to note here, that the inertia $I_n$, is the inertia of the system with no point mass.

The following b-values were found when fitting:

| Fit | b value |
|:---:|:---:|
| 1 | 0.1823 |
| 2 | 0.1809 |
| 3 | 0.179 |
| 4 | 0.1804 |
| 5 | 0.1815 |
| average | 0.18082 |

Table 2: b-values found from fitting 5 different graphs, using equation (15)

The gamma value can now be calculated:

$$\gamma = b \cdot 2 \cdot I_n = 0.18082 \cdot 2 \cdot \frac{1}{2} \cdot 0.12192\, kg \cdot (0.048\, m)^2 = 0.5 \cdot 10^{-4} kg \cdot m^2 \tag{16}$$

### 3.1.5   Amplitude ($A_0$)

The amplitude of the driving wave can be found by looking at the offset angle, meaning the driver is set level horizontally and the mass is adjusted to be in equilibrium at the top. The mass is then released, until it falls into a rest, in one of the potential wells. Then the driver is turned all the way vertical and the offset angle can be measured with the Pasco software. To get a more accurate value, this was done 5 times and an average was found:
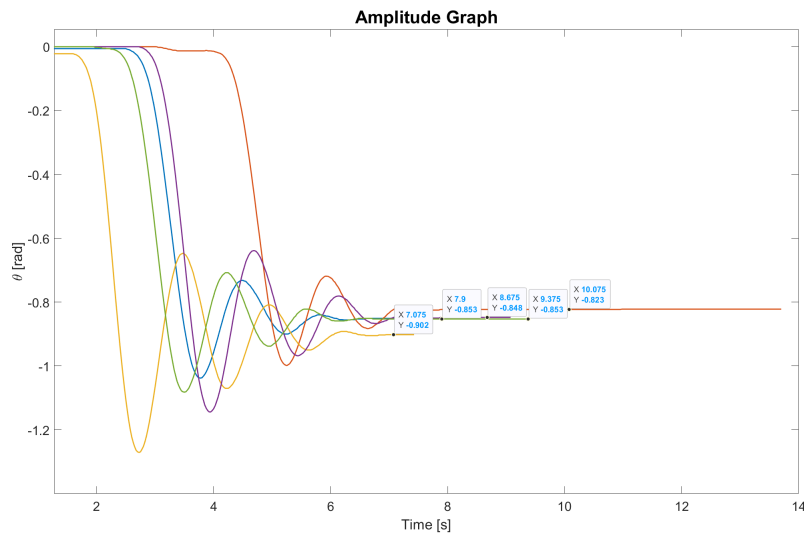


Figure 7: Amplitude graph

The amplitude is given by:

$$\theta_{offset} = \frac{A_0}{\kappa} \iff A_0 = \theta_{offset} \cdot \kappa \tag{17}$$

The average offset angle is first found to be:

$$\theta_{offset} = 0.8558 \, rad \tag{18}$$

The amplitude is now found using equation (17):

$$A_0 = 0.8558 \, rad \cdot 2.33 \cdot 10^{-3} \, N \cdot m \cdot rad^{-1} = 2 \cdot 10^{-3} N \cdot m \tag{19}$$

**Summary**

| Symbol | Value | Meaning |
|--------|-------|---------|
| $I$ | $1.7467 \cdot 10^{-4} kg \cdot m^2$ | Inertia |
| $\gamma$ | $5.0 \cdot 10^{-5} kg \cdot m^2$ | Damping coefficient |
| $\kappa$ | $2.33 \cdot 10^{-3} \frac{N \cdot m}{rad}$ | Spring constant |
| $m$ | $14.8502 \cdot 10^{-3} kg$ | Mass of lot |
| $g$ | $9.82 \frac{m}{s^2}$ | Gravitational constant |
| $r$ | $4.8 \cdot 10^{-2} m$ | Radius of disk |
| $A_0$ | $2.0 \cdot 10^{-3} N \cdot m$ | Amplitude of motor |
| $\omega_d$ | value vary | Angular frequency of motor |

Table 3: Summary of coefficient

## 3.2  Chaotic system

### 3.2.1  Matlab setup

The motion of the pendulum is described with a non-homogeneous nonlinear second order differential equation. The nonlinear element $sin(\theta)$, which comes from the mass in 8, makes the equation unable to be described with an exact solution, which is why in this report we will solve this numerically in Matlab.

To do this we need to represent the equations as two first order differential equations. We use the earlier described 'dot notation' and let variables x and y represent $\theta$ and $\dot{\theta}$ respectively. This corresponds to the following two first order differential equations:

$$\dot{x} = y \tag{20}$$

$$\dot{y} = \frac{A_0 cos(\omega_d t) + mgr sin(x) - \gamma y - \kappa x}{I} \tag{21}$$

These differential equations are used in MATLAB to simulate our torsion pendulum with the values of each coefficient found experimentally. This is done by using the ODE45 command, which integrates the differential equation over a set time interval (tspan) and initial conditions. For simplicity we set our initial conditions to $\theta(0) = 0$ and $\dot{\theta}(0) = 0$.

### 3.2.2   Angle plot

When working with the pendulum, looking at the 'angle plot' is properly the first thing anyone would look at. Which is a plot, showing how the angle changes over time. To analyze what is different when the point mass is added to the system, we first look at what happens with no mass, corresponding to harmonic oscillations. Therefore we expect the angle plot to have a periodic description. We can compare the phase plot we get from the setup with the simulation:
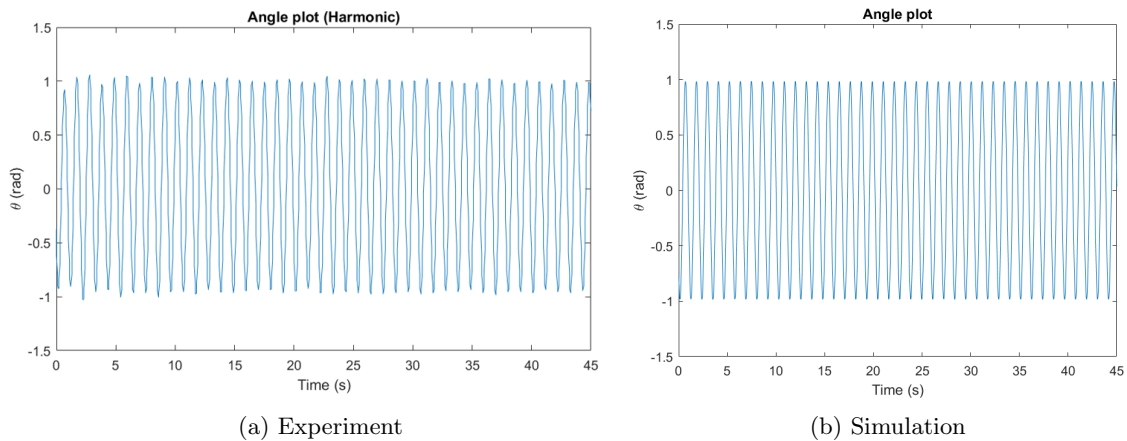


(a) Experiment        (b) Simulation

Figure 8: Angle plots showing harmonic oscillations

This shows clear periodic motion of the pendulum, as expected. Both the experiment and simulation, shows the exact same pattern, with only experimental errors as measuring uncertainties. Now when a mass is added and a nonlinear element is implemented in the system, chaotic motion is expected.
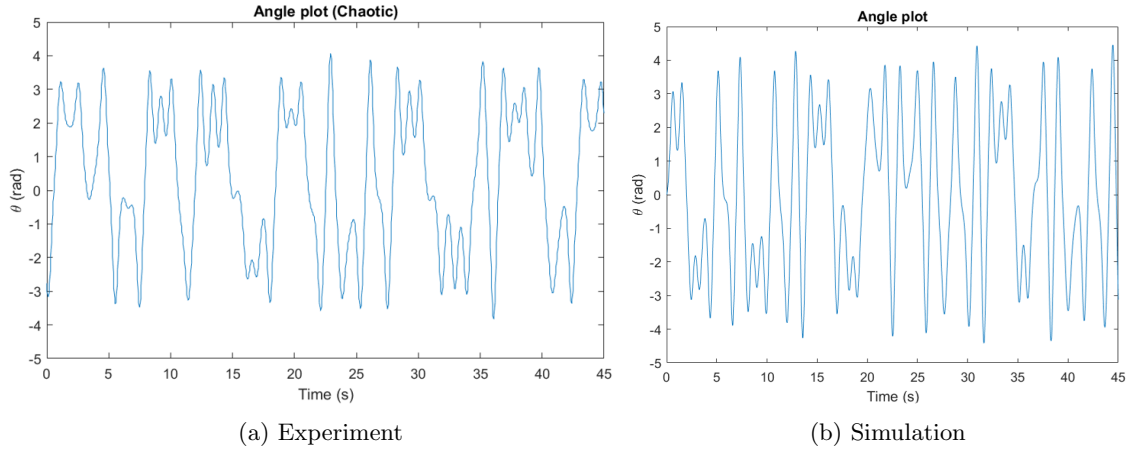
(a) Experiment

(b) Simulation

Figure 9: Angle plots showing chaotic oscillations

Looking at the angle plots in figure (9) a non repeating pattern, indicating a non-periodic motion is shown. Since it is non-periodic, the pattern is unpredictable. As seen from the experimental and simulated angle plot, they do not look the same at all. This is explained by the chaotic motion, since it is impossible to have the exact same initial conditions, resulting in vastly different angle plots. This shows that adding a mass to the system results in chaotic unpredictable motion, with clear comparability between experiment and simulations.

### 3.2.3   Phase space

When working with chaos, the phase space is often looked at, describing the different states that a system can occupy. For the pendulum, the state is described by the angle ($\theta$) and angular velocity ($\dot{\theta}$). Plotting these two against one another will give us a 'phase space diagram', also known as an attractor. The name attractor comes from the systems tendencies to converge to specific kinds of motion. There is different kinds of attractors. When working with chaotic systems the so called 'strange attractors' are analyzed, characterized by the non repeatable pattern in the phase space. For our system, it would be expected that the phase space would be moving around the two stationary point, mentioned earlier in relation the the potential graph. The following phase space is measured and simulated with and without the mass.
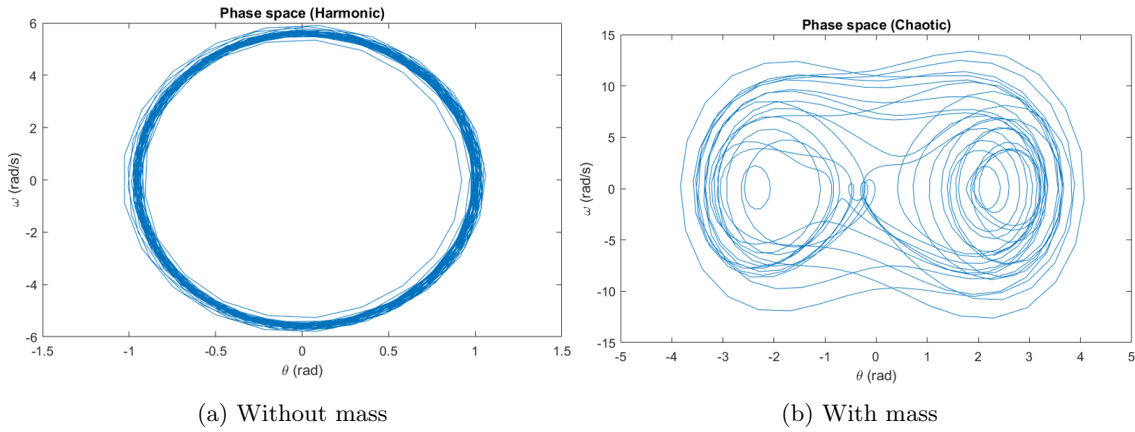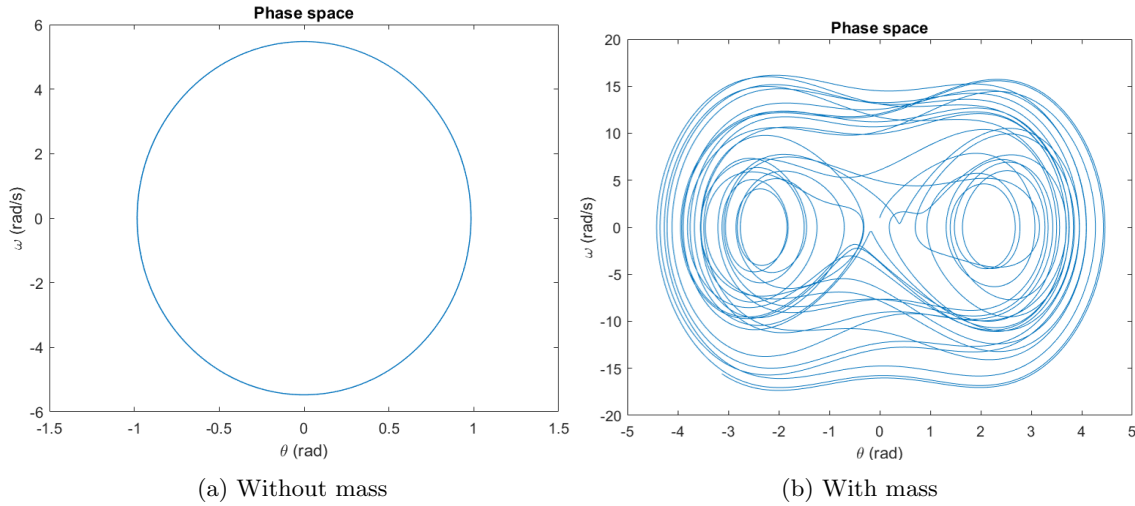
13

(a) Without mass

(b) With mass

Figure 10: Phase space of experiment



(a) Without mass

(b) With mass

Figure 11: Simulated phase space for tspan[0 100]

From figure (10) and (11) it is seen that for periodic motion when $m = 0$ the phase space illustrates circular pattern known as a limit cycle, as would be expected. But when looking at the phase space, when the mass is added, a more complex pattern emerges. The trajectories seem to move around in the so called strange attractor about the two stable stationary points. It is seen that the phase space acquired from the experiment is very similar to the simulation, indicating that the equation and coefficients align. It is clear to see now, that the experiment has limits on precision, but has the same overall shape as the simulation. This representation of the phase space diagrams may seem to contradict the fact, that the system never repeats for chaotic motion. Any two points can not have the same value, since it contradicts the idea of determinism. This may be obvious, since that would give multiple solutions for the same point. The reason this occurs for the phase space in figure (11) is due to the term $A_0 cos(\omega_d t)$, which introduces a third dimension to the system, namely time. The system oscillates back and forth in the z-axis which is not seen, since the diagram is a two dimensional representation of a three dimensional system. So it may seem

that the lines overlap, but in reality they occupy in two different z-coordinates. Chaos can not happen in two dimensions. We can not know the future state of an object purely on the basis of the current position, as this would require infinite precision. When looking at the phase diagram, over a longer period of time, the information in the strange attractor will decrease for longer period of time, since the phase diagram will get clotted, displaying only the shape of the strange attractor.

### 3.2.4  Poincaré plot

To extract more information from the pendulum, when driving for longer intervals we introduce what is called a 'Poincaré plot/diagram'. This limits our graph to only plot a point whenever our driving function ($A_0 cos(\omega_d t)$) performs a full rotation, corresponding to plotting the point every period $T = \frac{2\pi}{\omega_d}$. For periodic motion this will correspond to a point, but what is fascinating, is that when there is chaotic motion, The following diagrams are measured and simulated:
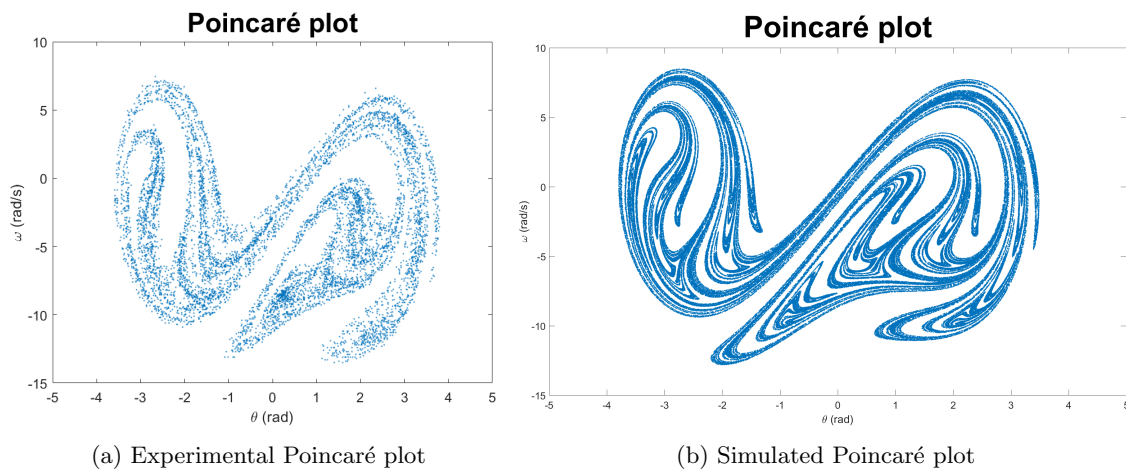


(a) Experimental Poincaré plot

(b) Simulated Poincaré plot

Figure 12: Pointcaré plots of experiment and simulation

We clearly see the same structure on the Poincaré plot for both the experiment and simulation. It is seen that they both look, as if they are constructed by a layer-like curved structure. Although they look very similar, we can also see differences between the two. There is seen a more developed Poincaré plot with more detailed lines, which is explained by the lack of error when simulating. The points in the experimental plot seem to be scattered, showing noise in the system. This noise is derived from errors that could have happened during the experiment, such as the setup tipping a little from side to side, due to the fast rotations of the disc. Another reason could be that the voltage output to the driver didn't end up being exactly the same during the whole experiment varying with $\pm 0.05V$. Manual errors are also found, since resetting the system requires that the point mass is in equilibrium at the top of the disc, which can be very difficult. Lastly an obvious error is also the Pasco software, rounding numbers to the nearest 100th, so that a grid pattern might be possible to interpret from figure (12a). All these errors cause the image to be more noisy and thus not giving the most clear Poincaré plot. The plots both show the same beautiful pattern,

again indicating that the simulation is able to explain the experiment

## 3.3  Fractals

One interesting feature of the Poincaré plot is that it resembles a fractal, that is, it does not resemble a perfect smooth shape. A fractal is a geometric shape, in an N-dimensional space, with its dimension corresponding to a non-integer fractal dimensionm, that is less than N. [5] This means that the pattern continues for arbitrarily small scales.
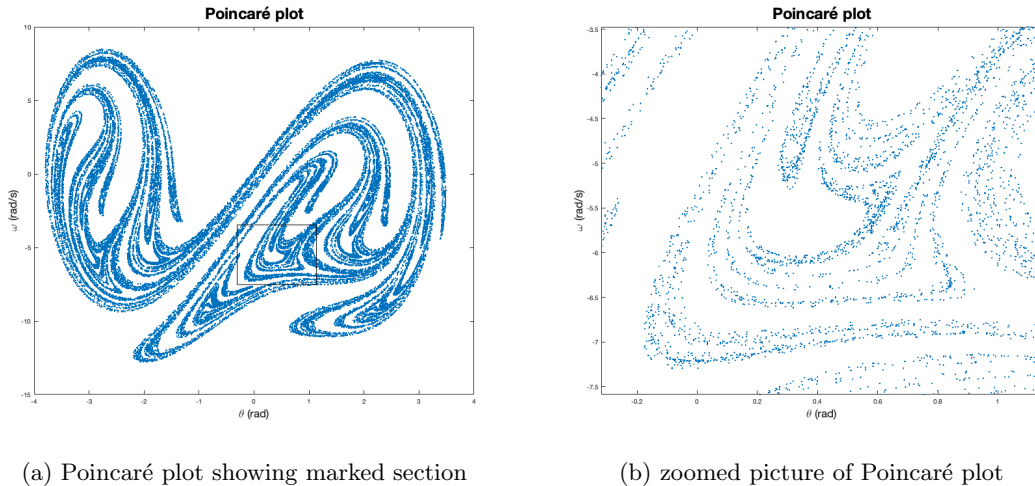


(a) Poincaré plot showing marked section



(b) zoomed picture of Poincaré plot

Figure 13: Poincaré zoom tspan[0 100000]

For our zoomed picture in figure (13b) we can see that the pattern continues even for a small scales supporting the claim, that the diagram has a non-integer dimension less than two. Imagine a continuous Poincaré-plot, we notice that this hypothetical diagram does not illustrate a perfect two-dimensional figure, as the diagram would continue to show pattern even for the smallest scales. This is due to the fact that no two points will lie exactly at the same place, as this would disprove the chaotic nature and lead to a periodic oscillation. [4] Imagine a two dimensional geometric figure, if one would zoom into this figure the same shape would continue as it is a perfectly smooth shape. Another way to look at it is imagining if one where to draw this hypothetical Poincaré plot by hand. Since the pattern continues indefinitely, it would seem as the figure has an infinite "perimeter" in a finite space and would be impossible to draw. Thus the figure most not have a perfectly smooth surface and can not have its dimension correspond to an integer value.

### 3.3.1  Boxcounting

When working with Poincaré plots and fractals, the fractal dimension of the systems is an obvious thing to analyze. The fractal dimension provides an index of determining the dimension of the system e.g. a periodic motion would have a fractal dimension of 1, as it is a line/curve in the phase space. This is very intuitive because a line only exist in one dimension, and for a plane the

dimension would simply be 2. This gives clear limitations of the fractal dimension of our system, since it must lie between 1 and 2. To find the fractal dimension, the method of boxcounting is used. The boxcounting method is used on the experimental and simulated Poincaré plots. The boxcounting method works by splitting the plot up in a grid pattern and examining the boxes that contain at least one data point. This is done for different grid patterns as illustarted:
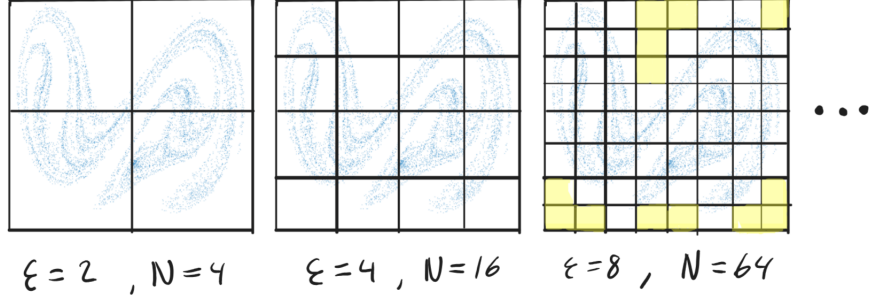


Figure 14: showing the approach of the boxcounting method with increasing $\epsilon$

By doing this we introduce different variables, namely 'N' for the total amount of boxes in the grid. And a value '$\epsilon$' representing the amount of boxes on each side. The amount of boxes including a valid data point, is given by $N(\epsilon)$ (visualized as the white boxes on figure (14)). The relation between $\epsilon$ and $N(\epsilon)$ will be given by:

$$N(\epsilon) = \epsilon^D \tag{22}$$

Where 'D' is given by the dimension of the given fractal. With this equation we can isolate D and get the following equation for the fractal dimension

$$D = \lim_{\epsilon \to \infty} \frac{log(N(\epsilon))}{log(\epsilon)} \tag{23}$$

From this we can see, that by plotting $log(N(\epsilon))$ as a function of $log(\epsilon)$ for different $\epsilon$ values, the dimension would be given by the slope of the resulting diagram. [6]

### 3.3.2 Comparison

For our specific system the Poincaré plots, for both experiment and theory, are analyzed as a 1024x1024 image. The image is converted to binary and the boxcount method shown on figure (14) is implemented, resulting in the following result:
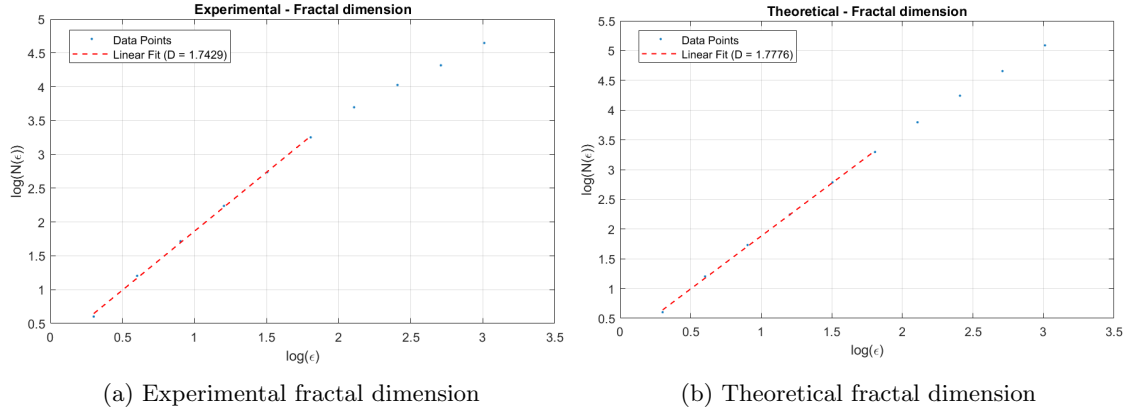
(a) Experimental fractal dimension

(b) Theoretical fractal dimension

Figure 15: Diagrams showing the fractal dimension of Poincaré plots

As it is seen from figure (15), only the first five data points is used as it is seen that the data seem to curve, indicating that it is not fully saturated. To prevent this more data from the Poincaré plots could be used, but would give practically the same results. From the result it is seen, that the fractal dimension of the system is found to be 1.7776 theoretically and 1.7429 experimentally. These values align with our prediction of being between 1-2, an seem to be very close, suggesting that the theory and experiment are in agreement. From these values, a difference can be represented with a value, for the first time in this report.

$$\frac{1.7776 - 1.7429}{1.7776} = 1.95\% \tag{24}$$

This error indicates that the complexity in the pattern of the experiment deviates by only 2%, from the theoretical value. again confirming that the simulation is a very good representation of the system.

## 3.4 Bifurcation diagram

When analyzing chaos in a non-linear dynamical system, it is interesting to look at the transition between periodic and chaotic behaviour. This is possible by choosing a parameter, and varying it. This will provide us with a Bifurcation diagram. By varying $\omega_d$, and plotting the values of angular velocity, as a function of $\omega_d$. Equivalent to compressing the Poincaré on one axis, and plotting it for the given $\omega_d$ value. Doing this we can accurately depict when the transition of chaos occurs, at a certain numerical value of $\omega_d$.
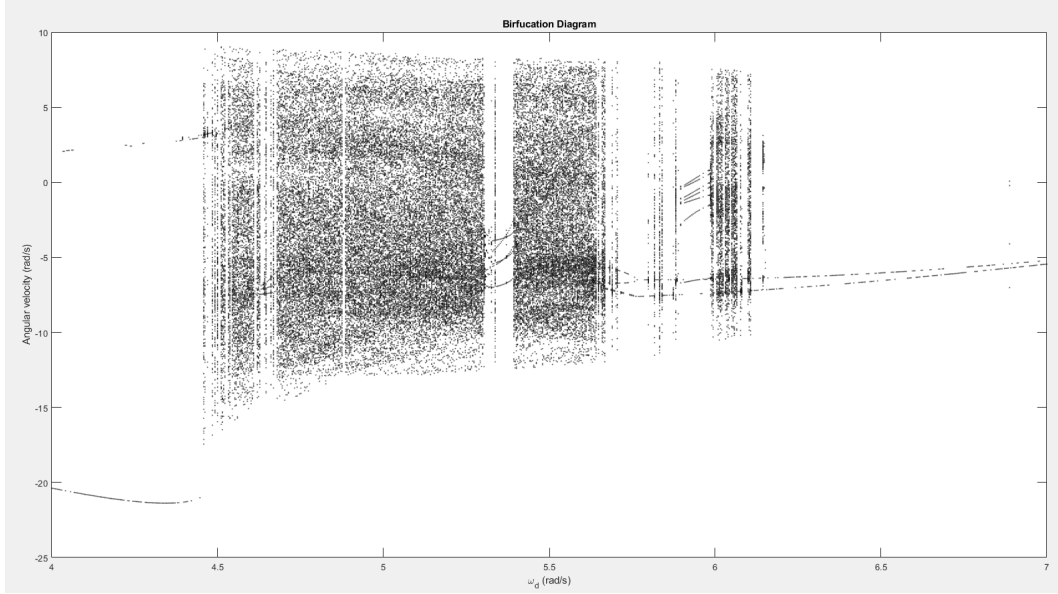
Figure 16: Bifurcation Diagram with $\omega_d$ varied from 4-7

Figure (16) shows the values of $\omega_d$ where we see clear signs of chaos and periodic behavior. From an $\omega_d$ value of 4 to about 4.5, the system is seen to behave in a periodic and non-chaotic manner, where the value of the angular velocity does not change for each full period. Whereas from values above 4.5, the values for angular velocity are scattered, indicating that the system will never repeat itself. Furthermore windows of periodicity are visible in the bifurcation diagram, where the system temporarily reverts back to periodic behaviour, and then returns to chaotic behaviour. These windows of periodicity, at values such as $\omega_d = 5.9 rad/s$, shows that the system cycles between multiple values of angular velocity, this would show a more complex wave in the angle plot but nevertheless still periodic compared to e.g. $\omega_d = 4.2 rad/s$ which would be a single sin wave.



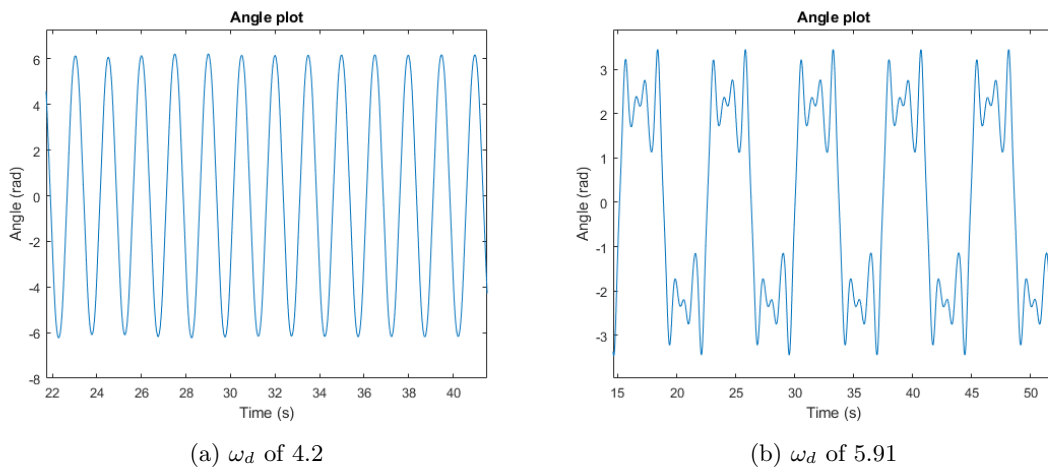(a) $\omega_d$ of 4.2

(b) $\omega_d$ of 5.91

Figure 17: Comparison of different periodic states shown with angle plots

It is important not to misinterpret, that multiple values of angular velocity for a certain value of

$\omega_d$ indicate, that the system is chaotic. As seen in figure (17b). It simply means that the angle plot is slightly more complex. Another thing to notice from the bifurcation diagram in figure (16), is that the angular velocity jumps from negative to positive, at values between $\omega_d = 4 \; rad/s$ and $\omega_d = 4.4 \; rad/s$. This is one of the many fascinating aspects derived from the bifurcation diagram, which makes is an incredible tool to examine how changing certain parameters affects the system as a whole.

### 3.4.1   Experimental bifurcation diagram

The bifurcation diagram in figure (16), is derived theoretically. we can not be sure, that the torsion pendulum would behave the exact same way. It is possible to create an experimental bifurcation diagram, since the pendulum can be driven with different values of $\omega_d$, and then plotting the data in a bifurcation diagram.



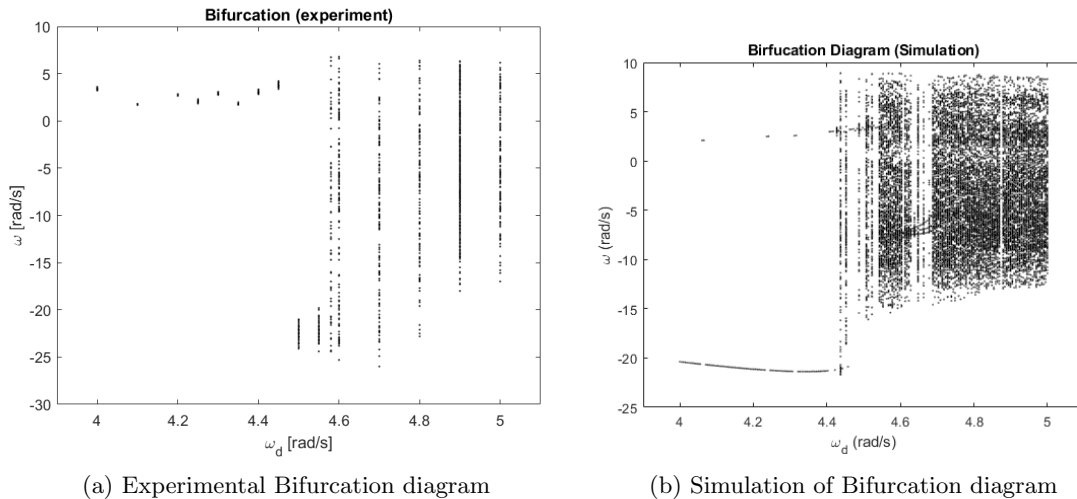(a) Experimental Bifurcation diagram          (b) Simulation of Bifurcation diagram

Figure 18: Comparison of experimental and simulated Bifurcation diagram with $\omega_d$ from 4-5 rad/s

By running several data collections of the pendulum at different $\omega_d$ values, it is possible to compare the behaviour of the pendulum to the simulation. The experimental bifurcation diagram closely matches the predicted behaviour from the simulation and analysis of the angle and Poincaré plot. Slight deviations are noticeable, such as the values of angular velocity in the lower values of $\omega_d$. These are due to the shape of the potential well in figure (3), where two stable points are achievable by the system, and thereby depending on the initial conditions, the system will tend towards one of them.

## 4   Conclusion

This report has shown that chaotic oscillation occurs simply by adding a mass to a torsion pendulum. This shows how easily a predictable system can be made into a complete new setup with

entirely different set of behaviours. By investigating the system and finding a corresponding phase space- and Poincaré diagram, this report shows that chaos is not purely random as one might think. Chaos conforms to a set of patterns, that unlocks a somewhat predictability. By looking at a mechanical system, we were able to derive a differential equation and find its corresponding parameters, which enables the system to be simulated and compared. By comparing the Poincaré plot of the experimental setup to the simulation and their corresponding fractal dimension, we notice that numerical solutions provide answers, that matches the data accurately. This tells us, that we can simulate the system and predict the general outcome, such as how the Poincaré will look. Showing that simulation is a useful tool even for systems, that may appear random. This can be applied to entirely different chaotic systems, that may not be measured as easily as a pendulum.

## 4.1   Perspective

Chaos is a lot more common than perfectly predictable systems. The weather is a good example of this, which is why weather reports are not always accurate. Weather predictions are made through differential equations, which are solved numerically. Here, the parameters are measured corresponding to the relevant term e.g. humidity, temperature, and winds etc. Numerous simulations are executed with parameters varying around the measured data, due to measurement uncertainties. With multiple simulations, a general tendency can be made, thereby giving the weather forecast.

The bifurcation diagram is an useful tool to test how certain parameters affect the system. This is why the weather in tropical places are a lot easier to predict compared to Nordic countries, as the parameters are set to make the system more predictable i.e. mostly sunny weather, whereas Nordic weather can significantly differ during a day.

## 4.2   Further research

For chaotic systems like the torsion pendulum, the sensitivity to initial condition would be interesting to investigate. Systems can vary in sensitivity to these initial conditions, to explain this the 'Lyapunov exponent' is introduced. This is a quantity in a dynamical system, that explains the rate, at which two different trajectories described by positions $x_1$ and $x_2$ will diverge or converge over some time 't'. The initial distance between these trajectories, is represented as '$\delta_0$'. This value will change over time depending on the different Lyapunov exponent. The distance at a given time can be expressed as:
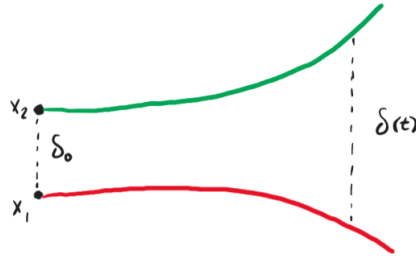
Figure 19: Diagram showing the divergence of initial condition $x_1$ and $x_2 = x_1 + \delta_0$

$$x_2(t) - x_1(t) = \delta(t) = \delta_0 \cdot e^{\lambda t} \tag{25}$$

From this it's possible to analyze, how fast the distance between $x_1$ and $x_2$ diverges or converges. The value of $\lambda$ describes how fast this process happens and depending on this value, it provides insight into the dynamics of the system:
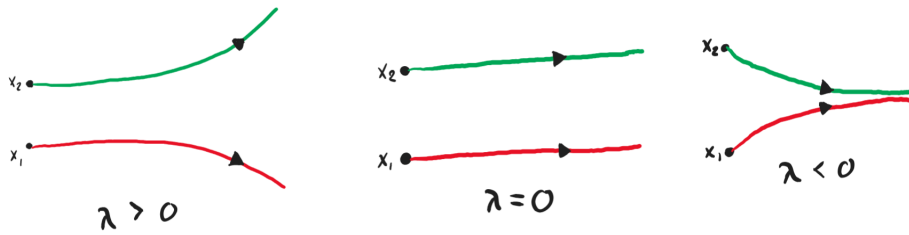


Figure 20: Diagram showing the different sign of the Lyapunov exponent

For chaotic behavior the Lyapunov exponent will vary from all the three states. Thus many different "strange attractors" can occur, where the behavior of the system can vary in complexity. This could be implemented to make a graph together with the bifurcation diagram, showing that the Lyapunov exponent is positive for chaotic behavior, negative for converging conditions and 0 for periodic behavior.

# List of symbols

| Symbol | Defenition | Unit |
|:---:|:---:|:---:|
| $I$ | Inertia | $N \cdot m$ |
| $I_n$ | Inertia with no added mass | $N \cdot m$ |
| $\theta$ | Angle | rad |
| $A_0$ | Amplitude | $N \cdot m$ |
| $\omega$ | Angular velocity | $\frac{rad}{s}$ |
| $\omega_d$ | Driving frequency | $\frac{rad}{s}$ |
| $\kappa$ | Torsion constant | $\frac{N \cdot m}{rad}$ |
| $\tau_d$ | Damping torque | $N \cdot m$ |
| $\tau_m$ | Driving torque | $N \cdot m$ |
| $\tau_s$ | Spring torque | $N \cdot m$ |
| $\tau_g$ | Gravitational torque | $N \cdot m$ |
| t | Time | s |
| $\alpha$ | Angular acceleration | $\frac{rad}{s^2}$ |
| $m_{disc}$ | Mass of disc | kg |
| $m$ | Mass of point mass | kg |
| $U_p$ | Potential energy | J |
| $U_e$ | Electric potential | V |
| $N$ | Total amount of boxes | No unit |
| $\epsilon$ | Amount of boxes on one side | No unit |
| $D$ | Fractal dimension | No unit |
| $\delta$ | Difference in value | No unit |
| $\lambda$ | Lyapunov exponent | No unit |

Table 4: List of symbols used in the report

# References

[1] Kirby, M.P., Schaller, N.C. and Torok, J.S. (1990) 'Visualization of strange attractors', in *Mathematical and Computer Modelling*, 14, pp. 395.

[2] Halliday, D. (2023) '15.5 DAMPED SIMPLE HARMONIC MOTION', in *Principles of Physics, Extended, International Adaptation*. 12th edn. Wiley Global Education , pp. 428–429.

[3] Mosekilde, E. Felsberg, R. (1994) *Ikke-lineær Dynamik og Kaos*

[4] Strogatz, S.H. (2024) '9.3 Chaos on a Strange Attractor', in *Nonlinear dynamics and chaos: with applications to physics, biology, chemistry, and engineering*. 2nd edn. Boca Raton, FL: CRC Press, pp. 326–327.

[5] Hoskin, P.W.O. (2000) '*Patterns of chaos: Fractal statistics and the oscillatory chemistry of Zircon*', Geochimica et Cosmochimica Acta, 64(11), pp. 1905–1906.

[6] Harrar, K. & Hamami, L. "The box counting method for evaluate the fractal Dimension in radiographic images", in 6th WSEAS International Conference on Circuits, Systems, Electronics, Control & Signal Pro cessing, Egypt, p. 385-389 (2007).

# Appendix

Code and data used for this report